Journal of Materials Chemistry A

COMMUNICATION

View Article Online
View Journal | View Issue

Cite this: J. Mater. Chem. A, 2018, 6, 22508

Received 4th July 2018
Accepted 31st October 2018

DOI: 10.1039/c8ta06418k

rsc.li/materials-a

Improved conversion efficiency of 10% for solid-state dye-sensitized solar cells utilizing P-type semiconducting CuI and multi-dye consisting of novel porphyrin dimer and organic dyes†

Naohiko Kato, *[a] Shinya Moribe,[a] Masahito Shiozawa,[a] Ryo Suzuki,[a] Kazuo Higuchi,[a] Akira Suzuki,[b] Mareedu Sreenivasu,[b] Katsuya Tsuchimoto,[b] Koji Tatematsu,[c] Katsuyoshi Mizumoto,[c] Shoichi Doi[c] and Tatsuo Toyoda[c]

To realize highly efficient solid-state dye-sensitized solar cells (SDSCs), the absorption range of the dye should be extended to the near-IR range to increase short-circuit current density (J_{sc}); a high J_{sc} in turn requires a highly conductive p-type semiconductor. A newly developed dye (**DIPDAB2**) with a porphyrin dimer structure provided higher absorption coefficients than the conventional dye with a similar framework (**DTBC**) in the long wavelength range of 700–800 nm, leading to higher incident photon-to-current conversion efficiencies. The dip in the absorption spectrum of **DIPDAB2** located at 500–700 nm between the Soret band and Q band was filled by combining with two kinds of organic dyes (**D131** and **D358**). The multi-dye consisting of the three dyes realized a high J_{sc} over 20 mA cm^{-2}. The use of copper iodide that has a higher conductivity than p-type organic semiconductors and copper complexes secured a high filling factor. Introduction of Li ions into the TiO_2 photoelectrodes improved the open-circuit voltage (V_{oc}) along with a slight increase in J_{sc}. Light soaking also contributed to a higher V_{oc}. The conversion efficiency of the present SDSC was as high as 10%.

1. Introduction

Dye-sensitized solar cells (DSCs) have various advantages of color choice and transparency, as well as low costs and low energy consumption in production,[1,2] compared with inorganic semiconductor-based solar cells. Using these unique characteristics, we have developed new application products such as light-emitting signboards, self-emitting guidance lights, *etc.*, in which DSCs are installed as stand-alone power sources.[3] Small-size DSCs provide a high conversion efficiency (η) of 14.7%.[4] However, η and durability are in a trade-off relationship, as summarized in Fig. S1†.[5–7] DSCs using a liquid electrolyte of a highly volatile solvent such as 3-methoxypropionitrile achieve a high η but suffer from low durability caused by solvent evaporation.[5] The use of γ-butyrolactone extends the lifetime up to 3–5 years in an outdoor environment, while it appreciably decreases η.[6] DSCs using ionic liquids are further durable; the lifetime estimated by an accelerated aging test is as long as 15 years.[7] However, η is further lower owing to low diffusivity of the redox ions in viscous ionic liquids. The liquid electrolytes raise another issue of DSC modules that wide sealants separating neighbouring cells are required for high durability, resulting in narrowing of active areas.

Replacement of the liquid electrolytes with solid-state p-type semiconductors can realize both high efficiency and high durability,[8,9] by solving the evaporation issue with securing a high hole conductivity. Therefore, studies on solid-state DSCs (SDSCs) have been very active. Table 1 summarizes electric properties of candidate p-type materials and photovoltaic properties of SDSCs. Among them, copper iodide (CuI) is highly conductive and stable.[10] The highest η of SDSCs using CuI is 7.4% coupled with the **N3** dye.[11] Although $CsSnI_3$ perovskite is also highly conductive and achieves a higher η of 8.5% with the **N719** dye,[12] it is an unstable material; easily oxidized under ambient air condition. On the other hand, conductivities of p-type organic semiconductors such as 2,2′,7,7′-tetrakis-(*N*,*N*-di-*p*-methoxyphenyl-amine)-9,9′-spirobifluorene (spiro-OMeTAD) and the copper complexes are much lower than those of the inorganic materials.[9,13–15]

In the present study, we have focused on four items to improve η of SDSCs. The priority for this purpose is to widen the absorption range of the dye to increase the short-circuit current density (J_{sc}). Therefore, the first item is a new dye (**DIPDAB2**) with a porphyrin dimer structure to achieve higher absorption coefficients in the near-IR range. A conventional indoline dye (**D149**) has a narrow absorption band ranging up to 780 nm,[16] resulting in a low J_{sc} of 13 mA cm^{-2}. We have developed **DIPDAB2** based on a donor–acceptor type porphyrin dimer dye: *N*-fused carbazole-zinc porphyrin-free-base porphyrin triad (**DTBC**) that sensitizes up to 900 nm.[17] The molecular structure

[a]Toyota Central Research and Development Laboratories, Inc., Nagakute-shi, Aichi 480-1192, Japan. E-mail: n-kato@mosk.tytlabs.co.jp
[b]AISIN Cosmos R&D Co.,Ltd., Kariya-shi, Aichi 448-8650, Japan
[c]AISIN SEIKI Co., Ltd., Kariya-shi, Aichi 448-8650, Japan

† Electronic supplementary information (ESI) available. See DOI: 10.1039/c8ta06418k

Table 1 Conductivity and valence band maximum (VBM) of candidate p-type materials, and photovoltaic properties of SDSCs

p-type conductor/dye	Conductivity [mS cm^{-1}]	VBM[a] [eV]	J_{sc} [mA cm^{-2}]	V_{oc} [V]	Filling factor	Efficiency [%]	Stability of p-type materials
CuI/D149[b]	308	−5.00	12.8	0.65	0.72	6.0	Stable
CuI/N3[c]	308	−5.00	14.5	0.73	0.70	7.4	Stable
CuI/D131 + **D358** + **DIPDAB2** (this work)	308	−5.00	22.0	0.65	0.71	10.1	Stable
$CsSnI_{2.95}F_{0.05}$ + 5% SnF_2/**N719**[d]	1111	−4.90	15.9	0.72	0.74	8.5	Unstable
Spiro-OMeTAD + Co complex **FK102/Y123**[e]	0.02	−5.20	9.5	0.98	0.77	7.2	Unstable
$Cu(dmp)_2TFSI$/**LEG4**[f]	0.10	−5.70	13.8	1.01	0.59	8.2	Stable
$Cu(tmby)_2TFSI$/**Y123**[g]	0.17	−5.67	13.9	1.08	0.73	11.0	Stable
$Cu(tmby)_2TFSI$/**WS72**[h]	0.17	−5.67	13.8	1.07	0.79	11.7	Stable

[a] Valence band maximum (VBM) was measured by photoelectron yield spectroscopy. [b] Ref. 22. [c] Ref. 11. [d] Ref. 12. [e] Ref. 13. [f] Ref. 9. [g] Ref. 14. [h] Ref. 15.

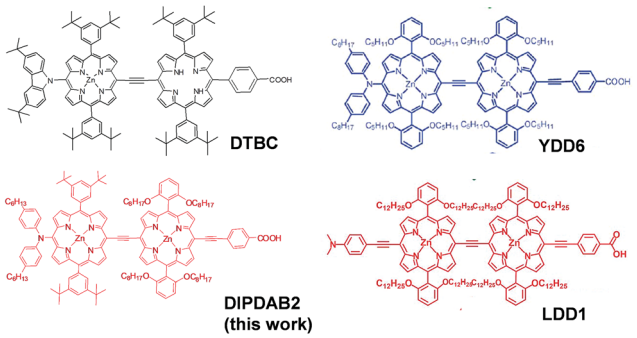

Fig. 1 Molecular structures of DTBC,[17] YDD6,[18] LDD1 (ref. 19) and DIPDAB2 dyes.

of **DIPDAB2** is compared with that of **DTBC** in Fig. 1. There are refinements in **DIPDAB2**. A stronger electron donor unit of bis(4-hexylphenyl)amine moiety and a π conjugated system extended by a triple-bond-connected acceptor of benzoic acid red-shift the Q band. **DTBC** and other dyes of the porphyrin dimer structures previously developed: **YDD6** (ref. 18) and **LDD1** (ref. 19) are equipped with common substituents on the two porphyrin rings as shown in Fig. 1. The unique point of **DIPDAB2** is that two different substituents are attached to the two porphyrin rings, which may inhibit aggregation of the dyes on the TiO_2 electrodes. The second is the use of a multi-dye consisting of **DIPDAB2** and two kinds of organic dyes: a yellow indoline dye (**D131**)[20] and a red indoline rhodanine dye (**D358**),[21] to cover a wide wavelength range from the visible to the near-IR. It has been demonstrated that co-sensitization can improve the performance of DSCs.[18,19] We have selected co-sensitizers of **D131** and **D358** dyes to match **DIPDAB2**.

A LiI treatment after the dye-absorption on the TiO_2 electrodes is employed to increase the open-circuit voltage (V_{oc}), which is the third item. The last is light soaking that also increases V_{oc}. The effects of the LiI treatment and light soaking on the present SDSCs are contrasting to those on liquid-type DSCs of improvements in J_{sc} with lowering in V_{oc}.

Another important point is the selection of the p-type semiconductor. CuI and copper complexes are stable materials and hence the candidates, as stated above. Our strategy of the improvement in η is to increase J_{sc}, which requires high conductivity of the p-type material, because detrimental impacts of the inner resistance are more notable at a higher J_{sc}. Copper complexes show high efficiency,[13–15] however, the conductivity is much lower than that of CuI. Therefore, we selected CuI for the p-type semiconductor. We have previously overcome the difficulties in filling the porous TiO_2 electrodes with CuI by using TiO_2 particles with a larger size than those for DSCs using liquid electrolytes, as shown in Fig. S2.†[22]

2. Experimental

2.1 Synthesis of DIPDAB2

We synthesized **DIPDAB2** dye by the scheme illustrated in Fig. S3.† The products were confirmed to be the target structure of **DIPDAB2**, by elemental analysis, ^{1}H-NMR, FT-IR, and MALDI-TOF-MS; see Fig. S4–S8.†

2.2 Fabrication of DSCs with a liquid electrolyte

To compare the sensitization performance of **DIPDAB2** with that of **DTBC**, DSCs using a liquid electrolyte were fabricated. Porous TiO_2 electrodes consisting of nanoparticles of *ca.* 20 nm in diameter were screen-printed on glass substrates covered with transparent conductive oxide (TCO) layers, followed by a surface treatment using a $TiCl_4$ aqueous solution. Then, the TiO_2 electrodes of 10 mm × 7 mm in size were immersed in a 0.2 mM dye (**DTBC** or **DIPDAB2**) and 2 mM chenodeoxycholic acid (**CDCA**) acetonitrile/*tert*-butyl alcohol (1 : 1) solution for 12 hours. The counter electrodes were prepared by chemical deposition of platinum onto the TCO glasses using a 0.05 M hexachloroplatinic acid solution at 400 °C. The dye-adsorbed TiO_2 electrodes and platinum counter electrodes were faced to each other with polyolefin-based sealants. An liquid electrolyte containing I^-/I_3^- redox couples using 0.6 M DMPII and 25 mM I_2, 0.1 M LiI and 0.5 M 4-*tert*-butylpyridine in acetonitrile was injected into the cells.

2.3 Fabrication of SDSCs with p-type semiconducting CuI

Double-layered TiO_2 electrodes were prepared by screen printing on the TCO glasses. The first layers of around 5 μm in

thickness were deposited using TiO_2 particles with a size distribution ranging from 35 nm to 400 nm. The average pore size was 160 nm. Larger TiO_2 particles of 400 nm in size were used for the 3 μm-thick second layers. The $TiCl_4$ post treatments were repeated three times. The TiO_2 electrodes of 10 mm × 7 mm in size were immersed in a 0.2 mM **DIPDAB2** dye and 2 mM **CDCA** acetonitrile/*tert*-butyl alcohol (1 : 1) solution for 1 hour, and then in 0.1 mM **D131** and 0.3 mM **D358** mixed ethanol solution for 16 hours. After the multi-dye adsorption, the TiO_2 electrodes were immersed into 0.1–0.5 M LiI acetonitrile solutions. Solid-state CuI was injected into the dye-adsorbed porous TiO_2 electrodes by dropping a CuI solution (CuI and 1-ethyl-3-methylimidazoliumthiocyanate in acetonitrile) followed by evaporation of the solvent as shown in S2.†[22–24] Finally, the TiO_2-dye-CuI electrodes were coupled with platinum foils as the counter electrodes to complete the SDSCs. SDSCs using **D149** were also fabricated for comparison. LiI concentration distribution in the SDSCs was analysed by time-of-flight secondary ion mass spectrometry (TOF-SIMS).

2.4 Evaluation of the photovoltaic performance

The current–voltage (*I*–*V*) characteristics of the DSCs were determined by measuring the photocurrent using an *I*–*V* tester (IV-9701, WACOM) under the simulated solar insolation of AM1.5G produced using a 1 kW xenon lamp and a 400 W halogen lamp (WXS-155S-L2, WACOM). The incident photon-to-current conversion efficiency (IPCE) was measured in a wavelength range of 300–900 nm using an equipment (CEP-2000, BUNKOU-KEIKI) specially designed for DSCs consisting of a xenon lamp, a monochromator, a digital lock-in amplifier, and a Keithley 2400 source meter.

3 Results and discussion

As mentioned above, at first we have designed and synthesized **DIPDAB2** with a porphyrin dimer structure to achieve higher absorption coefficients in the near-IR range than those of conventional **DTBC**.[17] UV-vis absorption spectra of **DIPDAB2** and **DTBC** adsorbed on porous TiO_2 films shown in Fig. 2 confirm the red-shifted Q band with higher absorbance of **DIPDAB2**. Comparison with the other porphyrin dimer dyes: **YDD6** (ref. 18) and **LDD1** (ref. 19) are summarized in Table S1.† The absorption coefficient of **DIPDAB2** at the Q band was much higher than that of **YDD6** and comparable with that of **LDD1**. Photovoltaic performance of the liquid DSCs are shown in Fig. 3 and Table S1.† The IPCE and conversion efficiency for **DIPDAB2** were much higher than those for **DTBC**, reflecting the notable enhancement in the absorbance. Similar trends were observed for **YDD6** (ref. 18) and **LDD1** (ref. 19) according to the absorption coefficients.

The second item is the use of a multi-dye. Although **DIPDAB2** exhibits high absorbance in the near-IR range as described above, there is a dip between the Soret band centered at 500 nm and the Q band located at around 700 nm. To fill the gap and secure highly efficient sensitization in the whole of the visible-near-IR range, a multi-dye consisting of **DIPDAB2** and two kinds of organic dyes: **D131** and **D358** was used. The molecular structures of **D131** and **D358** are displayed in Fig. S9.† Fig. 4 compares the IPCE spectrum of the SDSC using the multi-dye (**DIPDAB2** + **D131** + **D358**) with those for **D149** and **DIPDAB2**. **D131** and **D358** well complemented the dip between the Soret band and Q band originating from the porphyrin dimer in **DIPDAB2**. As a result, the IPCE spectrum for the multi-dye covered a notably wider range than that for **D149**, leading to a dramatic improvement in J_{sc} to over 20 mA cm^{-2} estimated from the IPCE spectrum. We consider that the multi-dye inhibits the aggregation of the single **DIPDAB2** dye.[18,19] As the result, the IPCE for the multi-dye in the absorption range of the Q band was much higher than the single **DIPDAB2** dye.

The third item is the post treatment using LiI. The dye-adsorbed TiO_2 electrodes were immersed in LiI acetonitrile solutions. Fig. 5 shows the *I*–*V* curves of the SDSCs with and

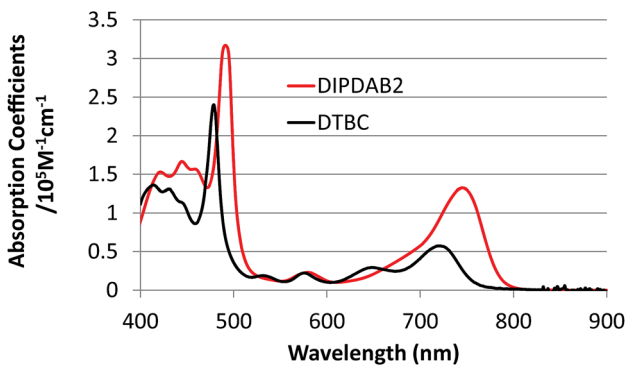

Fig. 2 UV-vis absorption spectra of **DIPDAB2** and **DTBC** adsorbed on porous TiO_2 films.

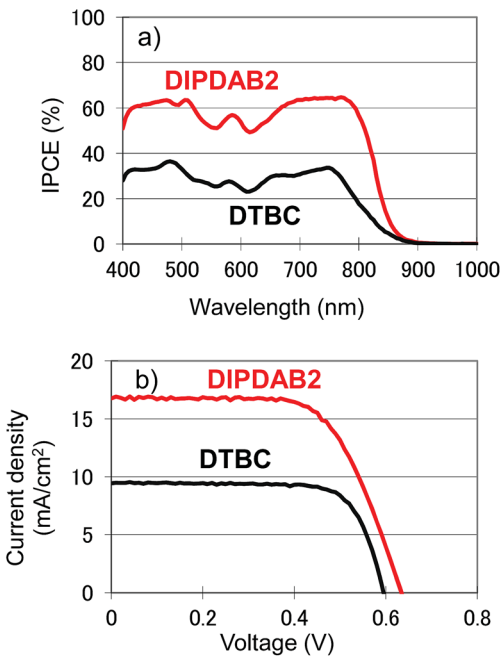

Fig. 3 (a) IPCE spectra, (b) current–voltage (*I*–*V*) curves under 1 sun irradiation of the liquid electrolyte DSCs using **DIPDAB2** and **DTBC**.

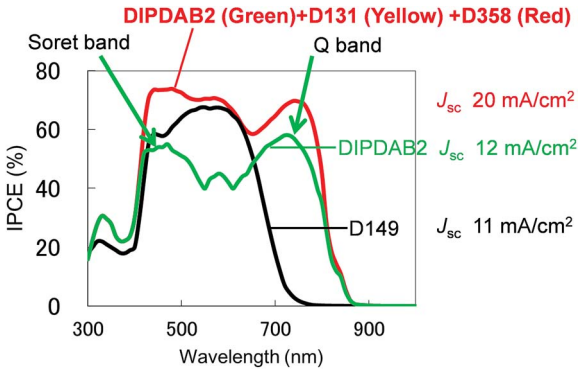

Fig. 4 IPCE spectra of the SDSCs using the multi-dye (**DIPDAB2** + **D131** + **D358**), **D149** and **DIPDAB2**.

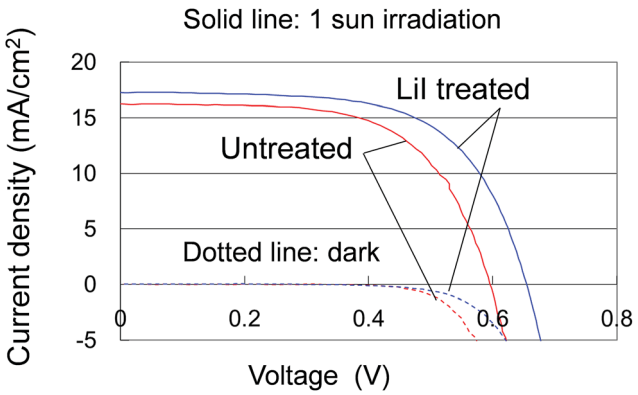

Fig. 5 Current–voltage (*I*–*V*) curves of the SDSCs under 1 sun irradiation and in the dark with and without the 0.5 M LiI post treatment.

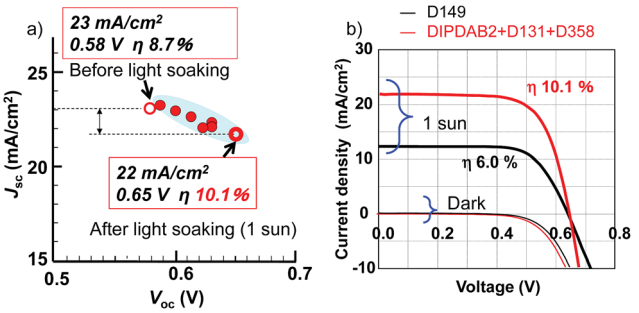

Fig. 6 (a) Relation between J_{sc} and V_{oc} of the SDSCs before/after the light soaking, (b) current–voltage (*I*–*V*) curves of the SDSCs under 1 sun irradiation using the multi-dye and **D149**.

without the post treatment. Time-of-flight secondary ion mass spectroscopy (TOF-SIMS) mappings of Li displayed in Fig. S10† revealed uniform distribution and higher concentrations of Li in the TiO_2 electrodes for higher concentrations of the LiI solutions. With increasing Li concentration, V_{oc} increased from 0.59 V for no LiI treatment, and eventually reached 0.65 V using the 0.5 M LiI solution with a slight increase in J_{sc}.

It is well known that introduction of LiI into an electrolyte consisting of I^-/I_3^- redox couples used for DSCs increases J_{sc} while it decreases V_{oc}.[25] Li ions adsorbed on the TiO_2 electrodes lowers the conduction-band minimum (CBM) of the TiO_2, leading to a higher efficiency of electron injection from the photo-excited dyes to the TiO_2 and consequently a higher J_{sc}. On the other hand, V_{oc} lowers as it is determined from the energy difference between the CBM of the TiO_2 and the redox level. The contrasting result of increasing V_{oc} for the present SDSCs suggests a different mechanism of the LiI treatment effect, like reduction of carrier recombination at the interfaces between the TiO_2 and CuI.

The fourth item is light soaking. During the light soaking at 1 sun, V_{oc} gradually increased with only a slight decrease in J_{sc}, as shown in Fig. 6a. After a half hour, V_{oc} reached 0.65 V (an improvement by 0.07 V) with securing a high J_{sc} of 22 mA cm^{-2} for the best-performance cell. The *I*–*V* curves of the SDSCs using the multi-dye and **D149** are compared in Fig. 6b. Reflecting the wider sensitivity range, J_{sc} for the multi-dye was much higher than that for **D149**. In addition, there was no degradation of the filling factor (FF) in spite of the higher J_{sc}, owing to the high conductivity of CuI. As a result, η for the multi-dye was significantly improved to be 10.1% compared with that for **D149**, and substantially exceeded the previously reported highest value of 7.4% using CuI and the **N3** dye.[11] The reproducibility was fairly good as summarized in Table S2.† It is worthy to note that the effect of the light soaking on the SDSCs were also contrasting to that of higher J_{sc} and lower V_{oc} on the DSCs using liquid electrolytes, although the present mechanism is not clear.

The photovoltaic performance of the SDSCs employing the four items is compared with previously reported ones in Table 1. The present J_{sc} of 22 mA cm^{-2} is extremely higher than those of the other SDSCs, with no remarkable degradation of FF compared with the other SDSCs using CuI. The disadvantage for CuI is lower V_{oc} than those for the other p-type semiconductors, caused by carrier recombination at the CuI surfaces.[26] It has been reported that CuI surfaces act as hole trapping sites.[26] The maximal V_{oc} determined from the difference between the CBM of TiO_2 (−4.2 eV from the vacuum level) and the VBM of CuI (−5.2 eV) is 1.0 V.[8] If V_{oc} could be improved to close to the ideal value with securing a high J_{sc} of 22 mA cm^{-2}, η of 15% would be attained. Thus, the SDSCs using the multi-dye consisting of the new porphyrin dimer dye **DIPDAB2** and organic dyes with CuI are promising for highly efficient and cost-effective solar cells.

4 Conclusions

We have established a strategy to improve the conversion efficiency of SDSCs; to widen the absorption range leading to a high current density and to use highly conductive p-type CuI for solid-state electrolytes. The multi-dye consisting of the newly developed **DIPDAB2** with a porphyrin dimer structure and two kinds of organic dyes (**D131** and **D358**) covered notably wider range with high IPCE compared with conventional porphyrin dimer dye **DTBC** and organic dyes, leading to an extremely high current density over 22 mA cm^{-2}. The CuI electrolyte fully injected into the porous TiO_2 electrodes secured a high FF. The LiI treatments to the dye-absorbed TiO_2 electrodes and light

soaking of the completed SDSCs improved V_{oc} with a slight increase in J_{sc}. Eventually, the conversion efficiency reached as high as 10%.

Conflicts of interest

There are no conflicts to declare.

Acknowledgements

We are grateful to Dr Yasuhiko Takeda and Prof. Tomoyoshi Motohiro for helpful discussion and suggestions. Dr Paidi Yella Reddy is acknowledged for the design of the novel porphyrin dimer dye.

Notes and references

1 B. O'Regan and M. Grätzel, *Nature*, 1991, **353**, 737.
2 M. Grätzel, *Acc. Chem. Res.*, 2009, **42**, 1788.
3 T. Miyasaka, *Trends and Topics in Sensitized and Organic Solar Cells*, CMC, Japan, 2012, ch. 3.
4 K. Kakiage, Y. Aoyama, T. Yano, K. Oya, J. Fujisawa and M. Hanaya, *Chem. Commun.*, 2015, **51**, 15894.
5 T. Toyoda, T. Sano, J. Nakajima, S. Doi, S. Fukumoto, A. Ito, T. Tohyama, M. Yoshida, T. Kanagawa, T. Motohiro, T. Shiga, K. Higuchi, H. Tanaka, Y. Takeda, T. Fukano, N. Katoh, A. Takeichi, K. Takechi and M. Shiozawa, *J. Photochem. Photobiol., A*, 2004, **164**, 203.
6 N. Kato, Y. Takeda, K. Higuchi, A. Takeichi, E. Sudo, H. Tanaka, T. Motohiro, T. Sano and T. Toyoda, *Sol. Energy Mater. Sol. Cells*, 2009, **93**, 893.
7 N. Kato, K. Higuchi, H. Tanaka, J. Nakajima, T. Sano and T. Toyoda, *Sol. Energy Mater. Sol. Cells*, 2011, **95**, 301.
8 K. Tennakone, *J. Phys. D: Appl. Phys.*, 1998, **31**, 1492.
9 M. Freitag, Q. Daniel, M. Pazoki, K. Sveinbjörnsson, J. Zhang, L. Sun, A. Hagfeldt and G. Boschloo, *Energy Environ. Sci.*, 2015, **8**, 2634.
10 D. Chen, Y. Wang, Z. Lin, J. Huang, X. Chen, D. Pan and F. Huang, *Cryst. Growth Des.*, 2010, **10**, 2057.
11 H. Sakamoto, S. Igarashi, M. Uchida, K. Niume and M. Nagai, *Org. Electron.*, 2012, **13**, 514.
12 I. Chung, B. Lee, J. He, R. P. H. Chang and M. G. Kanatzidis, *Nature*, 2012, **485**, 486.
13 J. Burschka, A. Dualeh, F. Kessler, E. Baranoff, N.-L. Cevey-Ha, C. Yi, M. K. Nazeeruddin and M. Grätzel, *J. Am. Chem. Soc.*, 2011, **133**, 18042.
14 Y. Cao, Y. Saygili, A. Ummadisingu, J. Teuscher, J. Luo, N. Pellet, F. Giordano, S. M. Zakeeruddin, J.-E. Moser, M. Freitag, A. Hagfeldt and M. Grätzel, *Nat. Commun.*, 2017, **8**, 15390.
15 W. Zhang, Y. Wu, H. W. Bahng, Y. Cao, C. Yi, Y. Saygili, J. Luo, Y. Liu, L. Kavan, J. E. Moser, A. Hagfeldt, H. Tian, S. M. Zakeeruddin, W. H. Zhu and M. Grätzel, *Energy Environ. Sci.*, 2018, **11**, 1779.
16 T. Horiuchi, H. Miura, K. Sumioka and S. Uchida, *J. Am. Chem. Soc.*, 2004, **126**, 12218.
17 Y. Liu, H. Lin, J. Ting Dy, K. Tamaki, J. Nakazaki, D. Nakayama, S. Uchida, T. Kubo and H. Segawa, *Chem. Commun.*, 2011, **47**, 4010.
18 H.-P. Wu, Z.-W. Ou, T.-Y. Pan, C.-M. Lan, W.-K. Huang, H.-W. Lee, N. M. Reddy, C.-T. Chen, W.-S. Chao, C.-Y. Yeh and E. W.-G. Diau, *Energy Environ. Sci.*, 2012, **5**, 9843.
19 J.-W. Shiu, Y.-C. Chang, C.-Y. Chan, H.-P. Wu, H.-Y. Hsu, C.-L. Wang, C.-Y. Lin and E. W.-G. Diau, *J. Mater. Chem. A*, 2015, **3**, 1417.
20 H. Tanaka, A. Takeichi, K. Higuchi, T. Motohiro, M. Takata, N. Hirota, J. Nakajima and T. Toyoda, *Sol. Energy Mater. Sol. Cells*, 2009, **93**, 1143.
21 M. Takata, *Introduction of photosensitive dyes for solar cells*, https://www.mpm.co.jp/electronic/solar-cells/index.html, 2018.
22 S. Moribe, A. Takeichi, J. Seki, N. Kato, K. Higuchi, K. Ueyama, K. Mizumoto and T. Toyoda, *Appl. Phys. Express*, 2012, **5**, 112302.
23 G. R. A. Kumara, A. Konno, K. Shiratsuchi, J. Tsukahara and K. Tennakone, *Chem. Mater.*, 2002, **14**, 954.
24 S. Moribe, N. Kato, K. Higuchi, K. Mizumoto and T. Toyoda, *Appl. Phys. Express*, 2017, **10**, 042301.
25 S. Pelet, J.-E. Moser and M. Grätzel, *J. Phys. Chem. B*, 2000, **104**, 1791.
26 V. P. S. Perera and K. Tennakone, *Sol. Energy Mater. Sol. Cells*, 2003, **79**, 249.

